Available online at www.sciencedirect.com
SCIENCE DIRECT®
International Journal of Solids and Structures 42 (2005) 3133–3146
INTERNATIONAL JOURNAL OF SOLIDS and STRUCTURES
www.elsevier.com/locate/ijsolstr

On the dynamic behavior of a functionally graded piezoelectric strip with periodic cracks vertical to the boundary

Jian Chen *, Zhengxing Liu

Department of Engineering Mechanics, Shanghai Jiaotong University, Huashan Road 1954, Shanghai 200030, PR China

Received 11 October 2004
Available online 23 November 2004

Abstract

The dynamic anti-plane problem for a functionally graded piezoelectric strip containing a periodic array of parallel cracks, which are perpendicular to the boundary, is considered. Integral transforms techniques are employed to reduce the problem to the solution of singular integral equations. Numerical results are presented to show the influences of geometry, electromechanical combination factor and material gradient parameter on the fracture behavior.

Keywords: Functionally graded material; Piezoelectricity; Fracture; Energy density factor

1. Introduction

Since piezoelectric materials are widely used as actuators and sensors in the smart and adaptive structures. To prevent failure during service and to secure the structural integrity of piezoelectric devices, understanding of the fracture behaviors of these materials become increasingly important. Up to now, a number of studies have been performed for the cracked piezoelectric materials (see e.g., Deeg, 1980; Pak, 1990; Sosa, 1991; Suo et al., 1992; Park and Sun, 1995; Sosa and Khutoryansky, 1996; Wang and Yu, 2000; Meguid and Chen, 2001; Kwon and Lee, 2001). Among these works, several scholars considered the fracture problem of periodic cracks in the homogeneous piezoelectric medium or along the interface of bimaterials (see, e.g., Gao and Wang, 2000; Hao, 2001; Gao et al., 2004). In order to adopt the complex function technique to analyze these problems, the periodical cracks are generally assumed to be collinear.

* Corresponding author. Tel.: +86 2168453022; fax: +86 2168453022.
E-mail address: chenjian130@yahoo.com.cn (J. Chen).

0020-7683/$ - see front matter © 2004 Elsevier Ltd. All rights reserved.
doi:10.1016/j.ijsolstr.2004.10.021

In addition, since the piezoelectric materials are generally brittle and susceptible to crack, in order to enhance the strength of piezoelectric devices and elongate their service life, the functionally graded piezoelectric materials (FGPMs), in which the material properties are continuously varied in one or more directions, have been developed (Wu et al., 1996; Zhu et al., 2000). Accordingly the fracture behaviors of FGPMs have become an intensive point. Wang and Noda (2001) discussed the fracture behavior of a cracked FGMP structure under the thermal load. Li and Weng (2002), Jin and Zhong (2002) considered the mode III Yoffe-type moving crack problem in a FGPM strip and in an infinite FGPM, respectively. Ueda (2003) solved the static mode III crack problem in a FGPM strip bonded to two elastic layers. Kwon (2003) studied the electrical nonlinear anti-plane shear crack in a FGPM strip. Chen et al. (2004) investigated the mixed mode crack problem in a FGPM plate.

In the past, several scholars studied the elastic problem of periodical cracks in functionally graded materials. For example, Erdogan and Ozturk (1995) studied the anti-plane problem of periodical cracks in functionally graded coatings. Choi (1997) investigated the problem of a periodical array of parallel cracks in a functionally graded medium under in-plane normal and shear load. However, to the authors' knowledge, few papers considered the solutions for the problem of periodical cracks in FGPM.

This paper considered the problem of a FGPM strip containing a periodical array of parallel cracks, which are perpendicular to the boundary. Integral transform technique is used to reduce the problem to the solution of singular integral equations. Numerical results are presented to discuss the possible fracture behaviors.

2. Formulation of problem

As shown in Fig. 1, a FGPM strip, which is transversely isotropic and poled in z-direction, contains the periodical cracks perpendicular to the boundary.

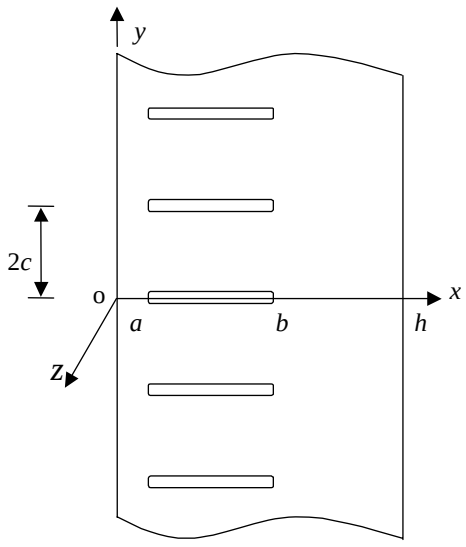

Fig. 1. Geometry of the crack problem.

The constitutive relations can be expressed as

$$\begin{aligned}\sigma_{zx} &= c_{44}\frac{\partial w}{\partial x} + e_{15}\frac{\partial \phi}{\partial x}, \quad D_x = e_{15}\frac{\partial w}{\partial x} - \varepsilon_{11}\frac{\partial \phi}{\partial x}, \quad E_x = -\frac{\partial \phi}{\partial x}\\ \sigma_{zy} &= c_{44}\frac{\partial w}{\partial y} + e_{15}\frac{\partial \phi}{\partial y}, \quad D_y = e_{15}\frac{\partial w}{\partial y} - \varepsilon_{11}\frac{\partial \phi}{\partial y}, \quad E_y = -\frac{\partial \phi}{\partial y}\end{aligned} \tag{1}$$

where w and ϕ are the mechanical displacement and electric potential; σ_{zk}, D_k, E_k $(k = x, y)$ are the components of anti-plane shear stresses, in-plane electric displacements and electric fields; c_{44}, ρ, e_{15}, ε_{11} are the shear modulus, mass density, piezoelectric coefficient and dielectric parameter, respectively.

It is assumed that the shear modulus, mass density, piezoelectric coefficient and dielectric parameter of FGPM coating vary smoothly according to exponential function along the thickness direction (e.g., Erdogan and Ozturk, 1995; Kwon, 2003). To make the analysis tractable, the focus is limited on a special class of FGPMs in which the variations of theses properties are in the same gradient.

Therefore,

$$c_{44} = c_{440}\mathrm{e}^{\beta x}, \quad e_{15} = e_{150}\mathrm{e}^{\beta x}, \quad \varepsilon_{11} = \varepsilon_{110}\mathrm{e}^{\beta x}, \quad \rho = \rho_0\mathrm{e}^{\beta x} \tag{2}$$

where c_{440}, ρ_0, e_{150}, ε_{110} are the material properties at $x = 0$. By introducing the Bleustein function (Bleustein, 1968) given by $\psi = \phi - (e_{150}/\varepsilon_{110})w$ in the form, the governing equations may be expressed as

$$\begin{aligned}&\nabla^2 w + \beta\frac{\partial w}{\partial x} = c_2^{-2}\frac{\partial^2 w}{\partial t^2}, \quad \nabla^2\psi + \beta\frac{\partial \psi}{\partial x} = 0\\ &\phi(x, y, t) = \frac{e_{150}}{\varepsilon_{110}}w(x, y, t) + \psi(x, y, t)\end{aligned} \tag{3}$$

where $\nabla^2 = \partial^2/\partial x^2 + \partial^2/\partial y^2$ is the two-dimensional Laplace operator, and the shear wave speed of the piezoelectric is

$$c_2 = \sqrt{\mu_0/\rho_0} \tag{4}$$

where $\mu_0 = c_{440} + e_{150}^2/\varepsilon_{110}$.

When the crack surfaces are assumed to be electrically permeable, it is found that the fracture behavior of piezoceramics will be independent of electrical loading (see, e.g., Wang and Yu, 2000), and this is contrary to many existing experimental results. Therefore, the electrically impermeable crack face condition is adopted here.

We will assume that through a superposition the problem is reduced to a local perturbation problem in which self-equilibrating crack surface tractions are the only non-vanishing external loads. Because of periodicity, it is sufficient to consider the problem for $0 < y < c$ only. Thus, the boundary and continuity conditions can be written as

$$w(x, c, t) = \phi(x, c, t) = 0, \quad 0 < x < h \tag{5}$$

$$\sigma_{zx}(0, y, t) = D_x(0, y, t) = 0, \quad 0 < y < c \tag{6}$$

$$\sigma_{zx}(h, y, t) = D_x(h, y, t) = 0, \quad 0 < y < c \tag{7}$$

$$\sigma_{zy}(x, 0, t) = \tau(x)H(t), \quad D_y(x, 0, t) = D(x)H(t), \qquad a < x < b \tag{8}$$

$$w(x, 0, t) = \phi(x, 0, t) = 0, \qquad 0 < x < a, \quad b < x < h \tag{9}$$

3. Integral equations

Let the Laplace transform pair be written as:

$$f^*(s) = \int_0^\infty f(t)\mathrm{e}^{-st}\,\mathrm{d}t, \quad f(t) = \frac{1}{2\pi\mathrm{i}}\int_{Br} f^*(s)\mathrm{e}^{st}\,\mathrm{d}s \tag{10}$$

in which Br stands for the Bromwich path of integration. The variable t in Eqs. (3) can be eliminated by the application of Eq. (10). By expressing the solution of Eqs. (3) in terms of the sums of finite and infinite Fourier transforms, it can be shown that

$$\begin{aligned}
w^*(x,y,s) &= \frac{1}{2\pi}\int_{-\infty}^{\infty}[A_1(\alpha,s)\mathrm{e}^{m_1 y} + A_2(\alpha,s)\mathrm{e}^{m_2 y}]\mathrm{e}^{-\mathrm{i}\alpha x}\,\mathrm{d}\alpha + \sum_1^\infty [B_{1k}(\gamma_k,s)\mathrm{e}^{p_{1k}x} + B_{2k}(\gamma_k,s)\mathrm{e}^{p_{2k}x}]\sin(\gamma_k y)\\
\psi^*(x,y,s) &= \frac{1}{2\pi}\int_{-\infty}^{\infty}[C_1(\alpha,s)\mathrm{e}^{n_1 y} + C_2(\alpha,s)\mathrm{e}^{n_2 y}]\mathrm{e}^{-\mathrm{i}\alpha x}\,\mathrm{d}\alpha + \sum_1^\infty [D_{1k}(\gamma_k,s)\mathrm{e}^{q_{1k}x} + D_{2k}(\gamma_k,s)\mathrm{e}^{q_{2k}x}]\sin(\gamma_k y)\\
\phi^*(x,y,s) &= \frac{e_{150}}{\varepsilon_{110}}w^*(x,y,s) + \psi^*(x,y,s)
\end{aligned} \tag{11}$$

where $A_{1,2}(\alpha,s)$, $B_{1k}(\gamma_k,s)$, $B_{2k}(\gamma_k,s)$, $C_{1,2}(\alpha,s)$, $D_{1k}(\gamma_k,s)$, and $D_{2k}(\gamma_k,s)$ are unknown functions to be determined and

$$\begin{aligned}
&m_1 = -m_2 = \sqrt{\alpha^2 + \mathrm{i}\beta\alpha + s^2/c_2^2}, \quad n_1 = -n_2 = \sqrt{\alpha^2 + \mathrm{i}\beta\alpha}, \quad \gamma_k = k\pi/c\\
&p_{1k} = -\beta/2 - \lambda_k, \quad p_{2k} = -\beta/2 + \lambda_k, \quad \lambda_k = \sqrt{\gamma_k^2 + \beta^2/4 + s^2/c_2^2}\\
&q_{1k} = -\beta/2 - \lambda_k', \quad q_{2k} = -\beta/2 + \lambda_k', \quad \lambda_k' = \sqrt{\gamma_k^2 + \beta^2/4}
\end{aligned} \tag{12}$$

From Eqs. (1), (2) and (11), the stresses and electric displacements are obtained as follows:

$$\begin{aligned}
\frac{\sigma_{zx}^*}{\mathrm{e}^{\beta x}} &= \frac{1}{2\pi}\int_{-\infty}^{\infty} -\mathrm{i}\alpha[\mu_0(A_1\mathrm{e}^{m_1 y} + A_2\mathrm{e}^{m_2 y}) + e_{150}(C_1\mathrm{e}^{n_1 y} + C_2\mathrm{e}^{n_2 y})]\mathrm{e}^{-\mathrm{i}\alpha x}\,\mathrm{d}\alpha\\
&\quad + \sum_1^\infty [\mu_0(B_{1k}p_{1k}\mathrm{e}^{p_{1k}x} + B_{2k}p_{2k}\mathrm{e}^{p_{2k}x}) + e_{150}(D_{1k}q_{1k}\mathrm{e}^{q_{1k}x} + D_{2k}q_{1k}\mathrm{e}^{q_{2k}x})]\sin(\gamma_k y)\\
\frac{\sigma_{zy}^*}{\mathrm{e}^{\beta x}} &= \frac{1}{2\pi}\int_{-\infty}^{\infty} [\mu_0(A_1 m_1\mathrm{e}^{m_1 y} + A_2 m_2\mathrm{e}^{m_2 y}) + e_{150}(C_1 n_1\mathrm{e}^{n_1 y} + C_2 n_2\mathrm{e}^{n_2 y})]\mathrm{e}^{-\mathrm{i}\alpha x}\,\mathrm{d}\alpha\\
&\quad + \sum_1^\infty [\mu_0(B_{1k}\mathrm{e}^{p_{1k}x} + B_{2k}\mathrm{e}^{p_{2k}x}) + e_{150}(D_{1k}\mathrm{e}^{q_{1k}x} + D_{2k}\mathrm{e}^{q_{2k}x})]\gamma_k\cos(\gamma_k y)\\
\frac{D_x^*}{\mathrm{e}^{\beta x}} &= \frac{1}{2\pi}\int_{-\infty}^{\infty} \mathrm{i}\alpha[\varepsilon_{110}(C_1\mathrm{e}^{n_1 y} + C_2\mathrm{e}^{n_2 y})]\mathrm{e}^{-\mathrm{i}\alpha x}\,\mathrm{d}\alpha + \sum_1^\infty [-\varepsilon_{110}(D_{1k}q_{1k}\mathrm{e}^{q_{1k}x} + D_{2k}q_{2k}\mathrm{e}^{q_{2k}x})]\sin(\gamma_k y)\\
\frac{D_y^*}{\mathrm{e}^{\beta x}} &= \frac{1}{2\pi}\int_{-\infty}^{\infty} [-\varepsilon_{110}(C_1 n_1\mathrm{e}^{n_1 y} + C_2 n_2\mathrm{e}^{n_2 y})]\mathrm{e}^{-\mathrm{i}\alpha x}\,\mathrm{d}\alpha + \sum_1^\infty [-\varepsilon_{110}(D_{1k}\mathrm{e}^{q_{1k}x} + D_{2k}\mathrm{e}^{q_{2k}x})]\gamma_k\cos(\gamma_k y)
\end{aligned} \tag{13}$$

Introducing the following functions

$$g_1(x,s)=\begin{cases}\dfrac{\partial w^*(x,0,s)}{\partial x} & a<x<b\\ 0 & x<a, x>b\end{cases},\quad g_2(x,s)=\begin{cases}\dfrac{\partial \phi^*(x,0,s)}{\partial x} & a<x<b\\ 0 & x<a,\quad x>b\end{cases} \tag{14}$$

and substituting Eqs. (11) into (14), from Eqs. (5) and (9) it follows that

$$\begin{aligned}
A_1(\alpha,s)&=-\frac{\mathrm{i}}{\alpha}\frac{\mathrm{e}^{m_2 c}}{\mathrm{e}^{m_1 c}-\mathrm{e}^{m_2 c}}\int_a^b g_1(u,s)\mathrm{e}^{\mathrm{i}\alpha u}\,\mathrm{d}u\\
A_2(\alpha,s)&=\frac{\mathrm{i}}{\alpha}\frac{\mathrm{e}^{m_1 c}}{\mathrm{e}^{m_1 c}-\mathrm{e}^{m_2 c}}\int_a^b g_1(u,s)\mathrm{e}^{\mathrm{i}\alpha u}\,\mathrm{d}u\\
C_1(\alpha,s)&=-\frac{\mathrm{i}}{\alpha}\frac{\mathrm{e}^{n_2 c}}{\mathrm{e}^{n_1 c}-\mathrm{e}^{n_2 c}}\int_a^b \left[-\frac{e_{150}}{\varepsilon_{110}}g_1(u,s)+g_2(u,s)\right]\mathrm{e}^{\mathrm{i}\alpha u}\,\mathrm{d}u\\
C_2(\alpha,s)&=\frac{\mathrm{i}}{\alpha}\frac{\mathrm{e}^{n_1 c}}{\mathrm{e}^{n_1 c}-\mathrm{e}^{n_2 c}}\int_a^b \left[-\frac{e_{150}}{\varepsilon_{110}}g_1(u,s)+g_2(u,s)\right]\mathrm{e}^{\mathrm{i}\alpha u}\,\mathrm{d}u
\end{aligned} \tag{15}$$

If we now substitute from Eqs. (13) and (15) into Eqs. (6) and (7) it can be shown that

$$\begin{aligned}
B_{1j}p_{1j}+B_{2j}p_{2j}&=-\frac{\gamma_j}{c\lambda_j}\int_a^b g_1(u,s)\mathrm{e}^{-p_{2j}u}\,\mathrm{d}u\\
D_{1j}q_{1j}+D_{2j}q_{2j}&=-\frac{\gamma_j}{c\lambda_j}\int_a^b \left[-\frac{e_{150}}{\varepsilon_{110}}g_1(u,s)+g_2(u,s)\right]\mathrm{e}^{-q_{2j}u}\,\mathrm{d}u\\
B_{1j}p_{1j}\mathrm{e}^{p_{1j}h}+B_{2j}p_{2j}\mathrm{e}^{p_{2j}h}&=-\frac{\gamma_j}{c\lambda_j}\int_a^b g_1(u,s)\mathrm{e}^{p_{1j}(h-u)}\,\mathrm{d}u\\
D_{1j}q_{1j}\mathrm{e}^{q_{1j}h}+D_{2j}q_{2j}\mathrm{e}^{q_{2j}h}&=-\frac{\gamma_j}{c\lambda_j}\int_a^b \left[-\frac{e_{150}}{\varepsilon_{110}}g_1(u,s)+g_2(u,s)\right]\mathrm{e}^{q_{1j}(h-u)}\,\mathrm{d}u
\end{aligned} \tag{16}$$

From Eqs. (16), the unknown B_{1j}, B_{2j}, D_{1j} and D_{2j} may then be obtained as follows:

$$\begin{aligned}
B_{1j}&=\frac{\gamma_j}{c\lambda_j p_{1j}(\mathrm{e}^{p_{1j}h}-\mathrm{e}^{p_{2j}h})}\int_a^b [\mathrm{e}^{p_{2j}(h-u)}-\mathrm{e}^{p_{1j}(h-u)}]g_1(u,s)\,\mathrm{d}u\\
B_{2j}&=\frac{\gamma_j}{c\lambda_j p_{2j}(\mathrm{e}^{p_{1j}h}-\mathrm{e}^{p_{2j}h})}\int_a^b [\mathrm{e}^{p_{1j}(h-u)}-\mathrm{e}^{p_{1j}h-p_{2j}u}]g_1(u,s)\,\mathrm{d}u\\
D_{1j}&=\frac{\gamma_j}{c\lambda'_j q_{1j}(\mathrm{e}^{q_{1j}h}-\mathrm{e}^{q_{2j}h})}\int_a^b [\mathrm{e}^{q_{2j}(h-u)}-\mathrm{e}^{q_{1j}(h-u)}]\left[-\frac{e_{150}}{\varepsilon_{110}}g_1(u,s)+g_2(u,s)\right]\mathrm{d}u\\
D_{2j}&=\frac{\gamma_j}{c\lambda'_j q_{2j}(\mathrm{e}^{q_{1j}h}-\mathrm{e}^{q_{2j}h})}\int_a^b [\mathrm{e}^{q_{1j}(h-u)}-\mathrm{e}^{q_{1j}h-q_{2j}u}]\left[-\frac{e_{150}}{\varepsilon_{110}}g_1(u,s)+g_2(u,s)\right]\mathrm{d}u
\end{aligned} \tag{17}$$

By substituting Eqs. (17) into Eqs. (13), we obtain

$$\begin{aligned}
\frac{\sigma^*_{zy}(x,0+,s)}{\mathrm{e}^{\beta x}}&=\frac{\tau(x)}{s\mathrm{e}^{\beta x}}\\
&=\lim_{y\to 0+}\frac{1}{\pi}\int_a^b\left\{[\mu_0(F_1+F_2)-\frac{e_{150}^2}{\varepsilon_{110}}(F'_1+F'_2)]g_1(u,s)+e_{150}(F'_1+F'_2)g_2(u,s)\right\}\mathrm{d}u\\
\frac{D^*_y(x,0+,s)}{\mathrm{e}^{\beta x}}&=\frac{D(x)}{s\mathrm{e}^{\beta x}}=\lim_{y\to 0+}\frac{1}{\pi}\int_a^b\{e_{150}(F'_1+F'_2)g_1(u,s)-\varepsilon_{110}(F'_1+F'_2)g_2(u,s)\}\,\mathrm{d}u
\end{aligned} \tag{18}$$

where

$$F_1(x,y,s,u)=\frac{1}{2}\int_{-\infty}^{\infty}\frac{\mathrm{i}}{\alpha}\frac{m_2\mathrm{e}^{m_1c+m_2y}-m_1\mathrm{e}^{m_2c+m_1y}}{\mathrm{e}^{m_1c}-\mathrm{e}^{m_2c}}\mathrm{e}^{\mathrm{i}\alpha(u-x)}\,\mathrm{d}\alpha$$
$$F_1'(x,y,s,u)=\frac{1}{2}\int_{-\infty}^{\infty}\frac{\mathrm{i}}{\alpha}\frac{n_2\mathrm{e}^{n_1c+n_2y}-n_1\mathrm{e}^{n_2c+n_1y}}{\mathrm{e}^{n_1c}-\mathrm{e}^{n_2c}}\mathrm{e}^{\mathrm{i}\alpha(u-x)}\,\mathrm{d}\alpha \tag{19}$$
$$F_2(x,y,s,u)=\frac{\pi}{c}\sum_{j=1}^{\infty}F_{2j}\cos(\gamma_j y),\quad F_2'(x,y,s,u)=\frac{\pi}{c}\sum_{j=1}^{\infty}F_{2j}'\cos(\gamma_j y)$$

and

$$F_{2j}=\frac{\gamma_j^2}{\lambda_j p_{1j}p_{2j}(\mathrm{e}^{p_{1j}h}-\mathrm{e}^{p_{2j}h})}\left\{p_{2j}\mathrm{e}^{p_{1j}x}\left[\mathrm{e}^{p_{2j}(h-u)}-\mathrm{e}^{p_{1j}(h-u)}\right]-p_{1j}\mathrm{e}^{p_{2j}x}\left[\mathrm{e}^{p_{1j}h-p_{2j}u}-\mathrm{e}^{p_{1j}(h-u)}\right]\right\}$$
$$F_{2j}'=\frac{\gamma_j^2}{\lambda_j' q_{1j}q_{2j}(\mathrm{e}^{q_{1j}h}-\mathrm{e}^{q_{2j}h})}\left\{q_{2j}\mathrm{e}^{q_{1j}x}\left[\mathrm{e}^{q_{2j}(h-u)}-\mathrm{e}^{q_{1j}(h-u)}\right]-q_{1j}\mathrm{e}^{q_{2j}x}\left[\mathrm{e}^{q_{1j}h-q_{2j}u}-\mathrm{e}^{q_{1j}(h-u)}\right]\right\} \tag{20}$$

Eqs. (18) would then provide the integral equation to evaluate $g_1(x,s)$ and $g_2(x,s)$. In order to determine the correct singularity of the unknown functions $g_1(x,s)$ and $g_2(x,s)$ and to develop an efficient method to solve the integral equations, the singular behavior of the kernels F_1, F_1', F_2 and F_2' must be examined. Note that for $\alpha\to\infty$ we have

$$m_1\to|\,\alpha\,|,\quad m_2\to-|\,\alpha\,|,\quad n_1\to|\,\alpha\,|,\quad n_2\to-|\,\alpha\,| \tag{21}$$

and then

$$F_1(x,y,s,u)=\frac{(u-x)}{(u-x)^2+y^2}+\frac{1}{2}\int_{-\infty}^{\infty}\frac{\mathrm{i}}{\alpha}\left[\frac{m_2\mathrm{e}^{m_1c+m_2y}-m_1\mathrm{e}^{m_2c+m_1y}}{\mathrm{e}^{m_1c}-\mathrm{e}^{m_2c}}+|\,\alpha\,|\,\mathrm{e}^{|\alpha y|}\right]\mathrm{e}^{\mathrm{i}\alpha(u-x)}\,\mathrm{d}\alpha$$
$$F_1'(x,y,s,u)=\frac{(u-x)}{(u-x)^2+y^2}+\frac{1}{2}\int_{-\infty}^{\infty}\frac{\mathrm{i}}{\alpha}\left[\frac{n_2\mathrm{e}^{n_1c+n_2y}-n_1\mathrm{e}^{n_2c+n_1y}}{\mathrm{e}^{n_1c}-\mathrm{e}^{n_2c}}+|\alpha|\mathrm{e}^{|\alpha y|}\right]\mathrm{e}^{\mathrm{i}\alpha(u-x)}\,\mathrm{d}\alpha \tag{22}$$

which, for $y\to 0$ becomes

$$F_1(x,0,s,u)=\frac{1}{u-x}+F_{1B}(x,0,s,u)$$
$$F_1'(x,0,s,u)=\frac{1}{u-x}+F_{1B}'(x,0,s,u) \tag{23}$$

where

$$F_{1B}(x,0,s,u)=\frac{1}{2}\int_{-\infty}^{\infty}\frac{\mathrm{i}}{\alpha}\left[\frac{m_2\mathrm{e}^{m_1c}-m_1\mathrm{e}^{m_2c}}{\mathrm{e}^{m_1c}-\mathrm{e}^{m_2c}}+|\,\alpha\,|\right]\mathrm{e}^{\mathrm{i}\alpha(u-x)}\,\mathrm{d}\alpha$$
$$F_{1B}'(x,0,s,u)=\frac{1}{2}\int_{-\infty}^{\infty}\frac{\mathrm{i}}{\alpha}\left[\frac{n_2\mathrm{e}^{n_1c}-n_1\mathrm{e}^{n_2c}}{\mathrm{e}^{n_1c}-\mathrm{e}^{n_2c}}+|\,\alpha\,|\right]\mathrm{e}^{\mathrm{i}\alpha(u-x)}\,\mathrm{d}\alpha \tag{24}$$

The kernels F_2 and F_2' are given in terms of infinite series. Therefore any singular behaviors F_2 and F_2' may have would be due to the asymptotic nature of these series. From Eqs. (12) it may be seen that for $j\to\infty$ we have

$$\lambda_j\to\gamma_j,\quad p_{1j}\to-\gamma_j,\quad p_{2j}\to\gamma_j,\quad \lambda_j'\to\gamma_j,\quad q_{1j}\to-\gamma_j,\quad q_{2j}\to\gamma_j \tag{25}$$

If we now let

$$F_2(x,y,s,u) = F_{2\infty}(x,y,s,u) + F_{2B}(x,y,s,u)$$
$$F'_2(x,y,s,u) = F'_{2\infty}(x,y,s,u) + F'_{2B}(x,y,s,u) \tag{26}$$

and use Eq. (25), the asymptotic series $F_{2\infty}$ and $F'_{2\infty}$ may be expressed as

$$F_{2\infty}(x,y,s,u) = F'_{2\infty}(x,y,s,u) = \frac{\pi}{c}\sum_{j=1}^{n} \mathrm{e}^{-\gamma_j(u+x)}\cos(\gamma_j y) = \frac{\pi}{c}\frac{\mathrm{e}^{\pi(u+x)/c}\cos(\pi y/c) - 1}{[\mathrm{e}^{\pi(u+x)/c} - \cos(\pi y/c)]^2 + \sin^2(\pi y/c)} \tag{27}$$

For $y = 0$, (27) becomes

$$F_{2\infty}(x,0,s,u) = F'_{2\infty}(x,0,s,u) = \frac{\pi}{c}\frac{1}{\mathrm{e}^{\pi(u+x)/c} - 1} \tag{28}$$

We further note that for small values of $(u + x)$ (28) has the following asymptotic form:

$$F_{2\infty}(x,0,s,u) = F'_{2\infty}(x,0,s,u) = \frac{1}{u+x} + \mathrm{O}(u+x) \tag{29}$$

Eqs. (18) may then be expressed as

$$\frac{\tau(x)}{s\mathrm{e}^{\beta x}} = \frac{1}{\pi}\int_a^b \left\{\left[\frac{c_{440}}{u-x} + \mu_0 k(u,x,s) - \frac{e_{150}^2}{\varepsilon_{110}}k'(u,x,s)\right]g_1(u,s) + e_{150}\left[\frac{1}{u-x} + k'(u,x,s)\right]g_2(u,s)\right\}\mathrm{d}u$$
$$\frac{D(x)}{s\mathrm{e}^{\beta x}} = \frac{1}{\pi}\int_a^b \left\{e_{150}\left[\frac{1}{u-x} + k'(u,x,s)\right]g_1(u,s) - \varepsilon_{110}\left[\frac{1}{u-x} + k'(u,x,s)\right]g_2(u,s)\right\}\mathrm{d}u \tag{30}$$

where

$$k(u,x,s) = F_{1B}(x,0,s,u) + F_{2B}(x,0,s,u) + F_{2\infty}(x,0,s,u)$$
$$k'(u,x,s) = F'_{1B}(x,0,s,u) + F'_{2B}(x,0,s,u) + F'_{2\infty}(x,0,s,u) \tag{31}$$

and

$$F_{2B}(x,0,s,u) = \frac{\pi}{c}\sum_{j=1}^{n}[F_{2j} - \mathrm{e}^{-\gamma_j(u+x)}], \quad F'_2(x,0,s,u) = \frac{\pi}{c}\sum_{j=1}^{n}[F'_{2j} - \mathrm{e}^{-\gamma_j(u+x)}] \tag{32}$$

The integral equations (30) will be solved for different crack types, that is, for internal crack and edge crack problem. To solve this integral equation for the case of an internal crack, one must also implement the single valuedness condition

$$\int_a^b g_1(u,s)\,\mathrm{d}u = 0, \quad \int_a^b g_2(u,s)\,\mathrm{d}u = 0 \tag{33}$$

Defining the following normalized quantities:

$$u = \frac{b-a}{2}\xi + \frac{b+a}{2}, \quad x = \frac{b-a}{2}\eta + \frac{b+a}{2}, \qquad -1 < (\xi,\eta) < 1$$
$$g_1(u,s) = \phi_1(\xi,s), \quad g_2(u,s) = \phi_2(\xi,s), \quad K(\xi,\eta,s) = \frac{b-a}{2}k(u,x,s), \quad K'(\xi,\eta,s) = \frac{b-a}{2}k'(u,x,s)$$
$$-\frac{\tau(x)}{\mathrm{e}^{\beta x}} = f_1(\eta), \quad -\frac{D(x)}{\mathrm{e}^{\beta x}} = f_2(\eta) \tag{34}$$

the integral equations (30) can be written to accommodate both internal and edge crack problem where $a = 0$

$$\frac{f_1(\eta)}{s} = \frac{1}{\pi}\int_a^b \left\{ \left[\frac{c_{440}}{\xi-\eta} + \mu_0 K(\xi,\eta,s) - \frac{e_{150}^2}{\varepsilon_{110}} K'(\xi,\eta,s)\right]\phi_1(\xi,s) + e_{150}\left[\frac{1}{\xi-\eta} + K'(\xi,\eta,s)\right]\phi_2(\xi,s)\right\} \mathrm{d}u$$

$$\frac{f_2(\eta)}{s} = \frac{1}{\pi}\int_a^b \left\{ e_{150}\left[\frac{1}{\xi-\eta} + K'(\xi,\eta,s)\right]\phi_1(\xi,s) - \varepsilon_{110}\left[\frac{1}{\xi-\eta} + K'(\xi,\eta,s)\right]\phi_2(\xi,s)\right\} \mathrm{d}u \tag{35}$$

For the internal crack problem, defining

$$\phi_1(\xi,s) = \frac{R(\xi,s)}{\sqrt{1-\xi^2}}, \quad \phi_2(\xi,s) = \frac{T(\xi,s)}{\sqrt{1-\xi^2}} \qquad -1 < \xi < 1 \tag{36}$$

and using the Lobatto–Chebyshev integration formula, the singular integral equations (35) and the single-valuedness condition (33) are reduced to an $2n \times 2n$ system of liner equations in terms of discrete values of $\phi_1(\xi_j,s)$ and $\phi_2(\xi_j,s)$ $(j = 1,\ldots,n)$ that are then solved numerically.

After determining $\phi_1(\xi,s)$ and $\phi_2(\xi,s)$ the stress intensity factors (SIFs) and electric displacement intensity factors (EDIFs) are determined as

$$\begin{aligned}
K^*_{\mathrm{III}}(a,s) &= \lim_{x\to a}\sqrt{2(x-a)}\sigma^*_{yz}(x,0,s) = \mathrm{e}^{\beta a}\sqrt{\frac{b-a}{2}}[c_{440}R(-1,s) + e_{150}T(-1,s)] \\
K^*_{\mathrm{III}}(b,s) &= -\lim_{x\to b}\sqrt{2(b-x)}\sigma^*_{yz}(x,0,s) = -\mathrm{e}^{\beta b}\sqrt{\frac{b-a}{2}}[c_{440}R(1,s) + e_{150}T(1,s)] \\
K^*_{\mathrm{D}}(a,s) &= \lim_{x\to a}\sqrt{2(x-a)}D^*_{y}(x,0,s) = \mathrm{e}^{\beta a}\sqrt{\frac{b-a}{2}}[e_{150}R(-1,s) - \varepsilon_{110}T(-1,s)] \\
K^*_{\mathrm{D}}(b,s) &= -\lim_{x\to b}\sqrt{2(b-x)}D^*_{y}(x,0,s) = \mathrm{e}^{\beta b}\sqrt{\frac{b-a}{2}}[e_{150}R(1,s) - \varepsilon_{110}T(1,s)]
\end{aligned} \tag{37}$$

Recently, some investigators found that the energy density factor (EDF) is an essential quantity for analyzing the piezoelectric crack growth behavior (Sih and Zuo, 2000; Zuo and Sih, 2000; Soh et al., 2001; Chen et al., 2004). For the anti-plane problem, the energy density factor is defined as

$$S_{\mathrm{III}} = \lim_{r\to 0}\frac{r}{2}(\tau_{zx}\varepsilon_{zx} + \tau_{zy}\varepsilon_{yx} + D_xE_x + D_yE_y) \tag{38}$$

in which r has been referred to as the core region within which microstructure effects become important. For the internal crack problem, EDF can be expressed in terms of SIF and EDIF as

$$\begin{aligned}
S_{\mathrm{III}}(a,t) &= \frac{1}{8\mu_0\mathrm{e}^{\beta a}}\left[K^2_{\mathrm{III}}(a,t) - \frac{e_{150}}{\varepsilon_{110}}K_{\mathrm{III}}(a,t)K_{\mathrm{D}}(a,t) + 2\frac{c_{440}}{\varepsilon_{110}}K^2_{\mathrm{D}}(a,t)\right] \\
S_{\mathrm{III}}(b,t) &= \frac{1}{8\mu_0\mathrm{e}^{\beta b}}\left[K^2_{\mathrm{III}}(b,t) - \frac{e_{150}}{\varepsilon_{110}}K_{\mathrm{III}}(b,t)K_{\mathrm{D}}(b,t) + 2\frac{c_{440}}{\varepsilon_{110}}K^2_{\mathrm{D}}(b,t)\right]
\end{aligned} \tag{39}$$

It can be easily found that EDF is always positive. For the pure mechanical case, EDF is equivalent to the traditional definition of energy release rate.

In the case of an edge crack at $x = 0$ the kernel $F_{2\infty}(x,0,s,u)$ and $F'_{2\infty}(x,0,s,u)$ are singular and with $1/(u-x)$ constitute a generalized Cauchy kernel. At this time, the unknown density function $\phi_1(\xi,s)$ and $\phi_2(\xi,s)$ can be expressed in the form

$$\phi_1(\xi,s)=\frac{R(\xi,s)}{\sqrt{1-\xi}}=\frac{R^*(\xi,s)}{\sqrt{1-\xi^2}},\quad \phi_2(\xi,s)=\frac{T(\xi,s)}{\sqrt{1-\xi}}=\frac{T^*(\xi,s)}{\sqrt{1-\xi^2}} \tag{40}$$

For this case, one should use $R^*(-1,s)=T^*(-1,s)=0$ instead of the single-valuedness conditions. Now SIF and EDIF are determined as

$$\begin{aligned} K^*_{\mathrm{III}}(b)&=-\lim_{x\to b}\sqrt{2(b-x)}\sigma^*_{yz}(x,0,p)=-\mathrm{e}^{\beta b}\sqrt{b}[c_{440}R(1,p)+e_{150}T(1,p)]\\ K^*_{\mathrm{D}}(b)&=-\lim_{x\to b}\sqrt{2(b-x)}D^*_{y}(x,0,p)=\mathrm{e}^{\beta b}\sqrt{b}[e_{150}R(1,p)-\varepsilon_{110}T(1,p)] \end{aligned} \tag{41}$$

and EDF can be expressed as

$$S_{\mathrm{III}}(b,t)=\frac{1}{8\mu_0\mathrm{e}^{\beta b}}\left[K^2_{\mathrm{III}}(b,t)-\frac{e_{150}}{\varepsilon_{110}}K_{\mathrm{III}}(b,t)K_{\mathrm{D}}(b,t)+2\frac{c_{440}}{\varepsilon_{110}}K^2_{\mathrm{D}}(b,t)\right] \tag{42}$$

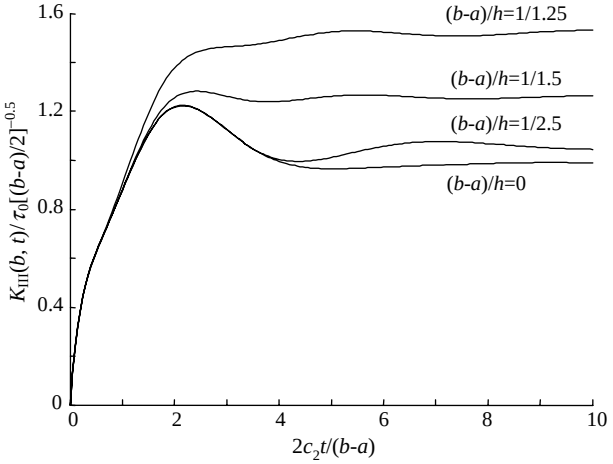

Fig. 2. Dynamic SIF for a homogeneous piezoelectric strip with only a central crack ($(b+a)=c$) under only shear impact ($\lambda=0$).

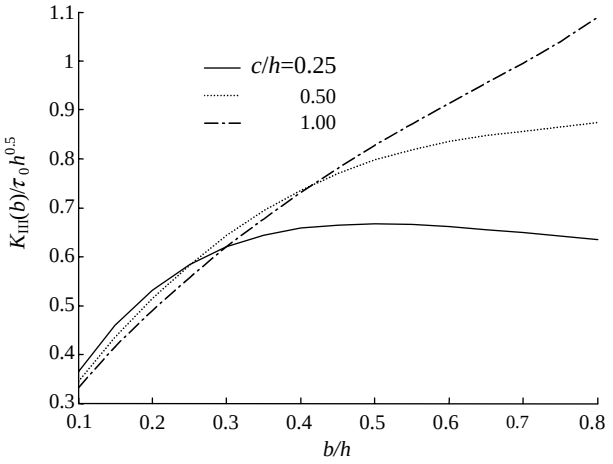

Fig. 3. Static SIF for the periodically edge-cracked piezoelectric strip ($\lambda=0$, $\beta h=\ln(0.5)$).

4. Numerical results

In this section, we investigate the transient response of periodically cracked FGPM strip. It is assumed that the material at $x = 0$ are $BaTiO_3$, whose material constants are $c_{440} = 4.4 \times 10^{10}\,\mathrm{N/m^2}$, $e_{150} = 11.4\,\mathrm{C/m^2}$, $\varepsilon_{110} = 128.3 \times 10^{-10}\,\mathrm{C/Vm}$, $\rho_0 = 7.5 \times 10^3\,\mathrm{kg/m^3}$. The periodical cracks are assumed to be subjected to uniform shear impact $\tau_0 H(t)$ and uniform electric displacement loading $D_0 H(t)$. The electromechanical coupling factor λ is defined as $\lambda = D_0 e_{150}/(\tau_0 \varepsilon_{110})$ to reflect the combination between the shear impact $\tau_0 H(t)$ and electrical impact $D_0 H(t)$.

It can be easily found that, if $c/h \to \infty$ the numerical results will approach the general results of a piezoelectric strip with only a crack. Fig. 2 shows the dynamic SIF of a piezoelectric strip with a central crack

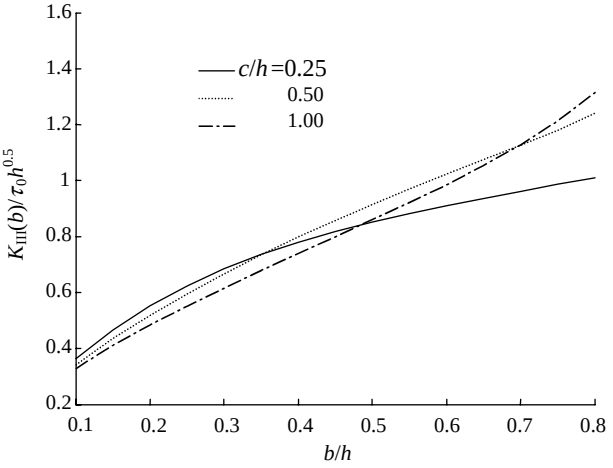

Fig. 4. Static SIF for the periodically edge-cracked piezoelectric strip ($\lambda = 0$, $\beta h = \ln(2.0)$).

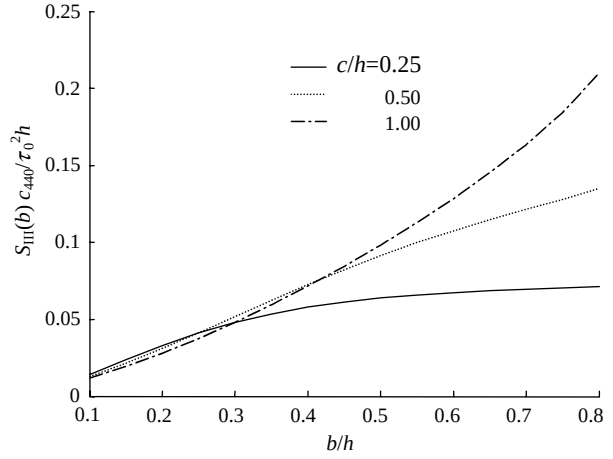

Fig. 5. Static EDF for the periodically edge-cracked piezoelectric strip ($\lambda = 0$, $\beta h = \ln(0.5)$).

under only shear impact (in the numerical analysis, $c/h = 10$), and they are in good agreement with those given by Wang and Yu (2000).

Compared to the internal crack problem, the surface crack problem is more practical. Then, all results presented in the following part are presented for $a = 0$ (i.e., the surface crack problem). Note that in the following part k_{III} is normalized with respect to a constant $\tau_0 h^{0.5}$ rather than the traditional factor $\tau_0 b^{0.5}$. At the same time, S_{III} is normalized with respect to a constant $\tau_0^2 h/c_{440}$.

Figs. 3 and 4 show the static SIF for the periodically edge-cracked piezoelectric strip under only shear impact. It can be found that k_{III} decreases with decreasing c/h and approaches zero as $c/h \to 0$. For the case of $\beta h > 0$, k_{III} increases with increasing crack length b/h. For the case of $\beta h < 0$, if the crack span c/h is very small (such as $c/h = 0.25$), k_{III} first increases, goes through a maximum and then decreases. Since the material properties at the different crack tip are variable, the increase or decrease of k_{III} does not always decide

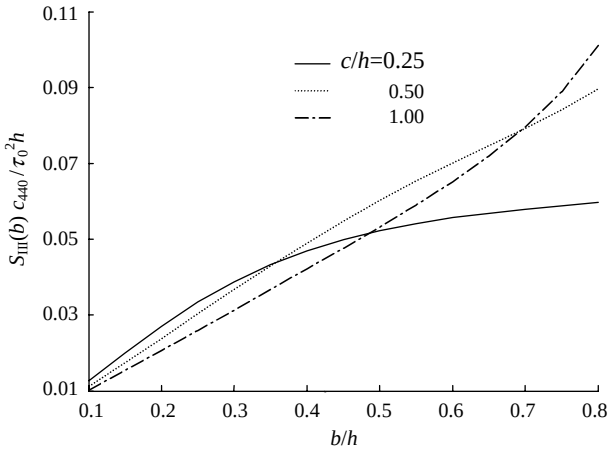

Fig. 6. Static EDF for the periodically edge-cracked piezoelectric strip ($\lambda = 0$, $\beta h = \ln(2.0)$).

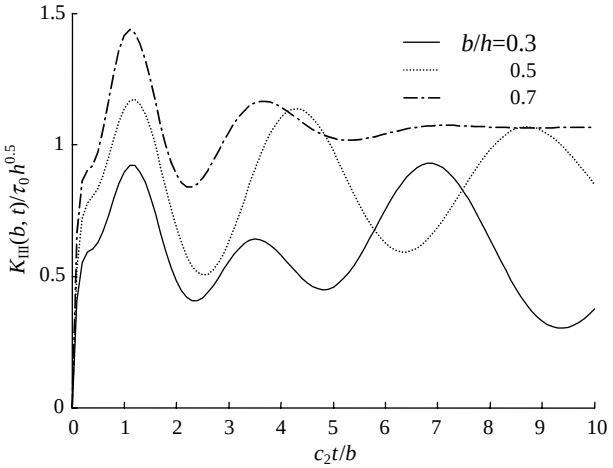

Fig. 7. Effect of b/h on dynamic SIF for the periodically edge-cracked piezoelectric strip ($\lambda = -0.2$, $c/h = 1.0$, $\beta h = \ln(1.0)$).

the crack propagation. As shown in Figs. 5 and 6, the static EDF always increases with increasing crack length b/h, and it means that the crack is easier to propagate as the crack length increases.

Figs. 7 and 8 show the effect of crack length b/h and crack span c/h on the dynamic SIF, respectively. As the crack length is very large (such as $b/h = 0.7$), the boundary effects will dominate the dynamic SIF, and the dynamic SIF approaches the corresponding static value in a short time. With the decrease of crack span c/h, the oscillating cycle of dynamic SIF increases due to the wave propagation and diffraction between the periodical cracks.

It is found that, under the combined loading, λ has insignificant effect on the normalized EDIF $K_D(b,t)/D_0h^{0.5}$. However, as shown in Figs. 9 and 10, the electric impact plays a great role in the transient fracture behavior. First, the applied direction of electric impact will lead to an increase or decrease in the resulting dynamic SIF at different loading stages. Second, according to the criterion of energy density factor, the electric impact always enhances the crack extension in the piezoelectric $BaTiO_3$ strip. Third, the peak value of

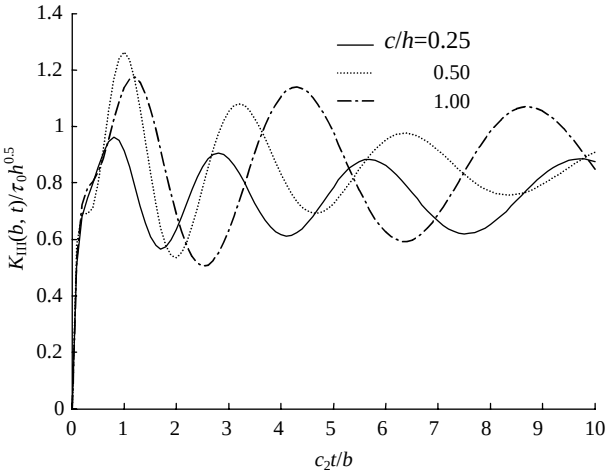

Fig. 8. Effect of c/h on dynamic SIF for the periodically edge-cracked piezoelectric strip ($\lambda = -0.2$, $b/h = 0.5$, $\beta h = \ln(1.0)$).

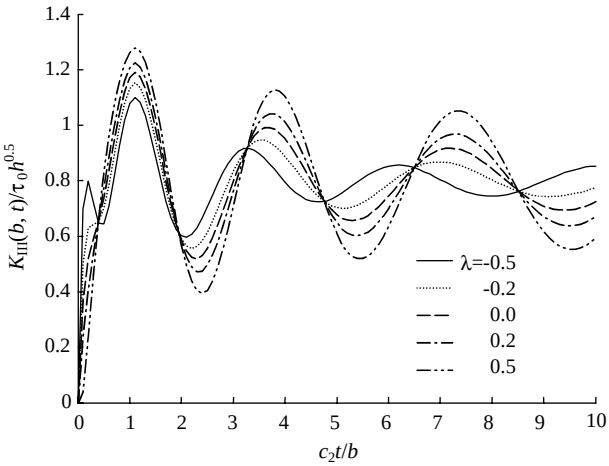

Fig. 9. Effect of λ on dynamic SIF for the periodically edge-cracked piezoelectric strip ($c/h = 0.5$, $b/h = 0.5$, $\beta h = \ln(0.5)$).

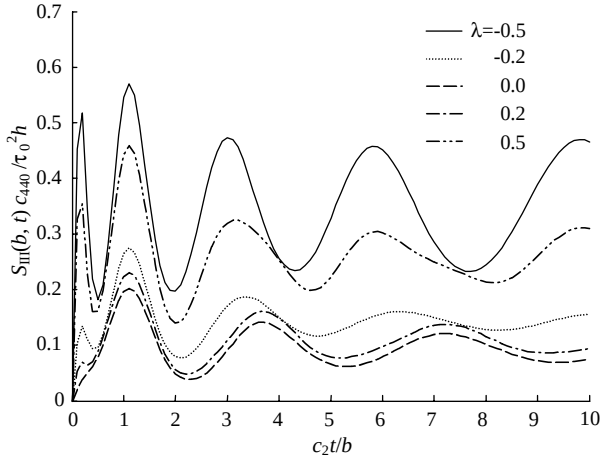

Fig. 10. Effect of λ on dynamic EDF for the periodically edge-cracked piezoelectric strip ($c/h = 0.5$, $b/h = 0.5$, $\beta h = \ln(0.5)$).

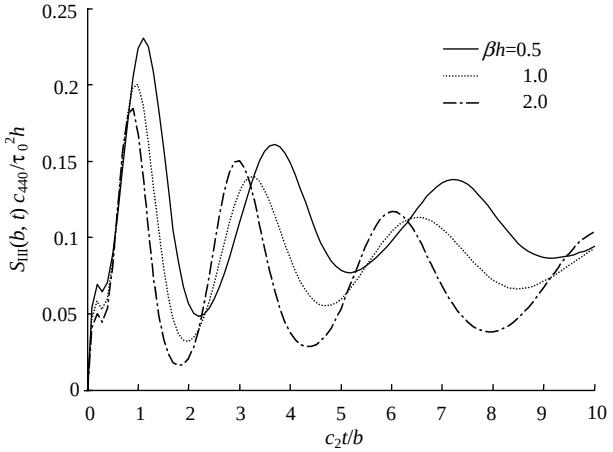

Fig. 11. Effect of βh on dynamic EDF for the periodically edge-cracked piezoelectric strip ($c/h = 0.5$, $b/h = 0.5$, $\lambda = 0.2$).

EDF under the negative electric loading is always higher than that under the positive electric loading, and it means that the crack is more likely to propagate under the negative electric loading than under the positive one.

Fig. 11 illustrates the influence of material gradient parameter βh on dynamic EDF. It can be found that, the peak values of normalized EDF decrease with the increase of βh, and this means that the increase of βh could impede the crack extension.

Acknowledgments

This work is supported by the National Natural Science Foundation of China through Grant No. 10132010 and 10302020.

References

Bleustein, J.L., 1968. A new surface wave in piezoelectric materials. Applied Physics Letters 13, 412–413.
Chen, J., Liu, Z.X., Zou, Z.Z., 2004. Crack initiation behavior of functionally graded piezoelectric material: prediction by the strain energy density criterion. Theoretical and Applied Fracture Mechanics 41, 63–82.
Choi, H.J., 1997. A periodic array of cracks in a functionally graded nonhomogeneous medium loaded under in-plane normal and shear. International Journal of Fracture 88, 107–128.
Deeg, W.F., 1980. Analysis of dislocation crack and inclusion problems in piezoelectric solids. PhD Dissertation, Standford University.
Erdogan, F., Ozturk, M., 1995. Periodic cracking of functionally graded coatings. International Journal of Engineering Science 33 (15), 2179–2195.
Gao, C.F., Wang, M.Z., 2000. Collinear permeable cracks between dissimilar piezoelectric materials. International Journal of Solids and Structures 37, 4969–4986.
Gao, C.F., Hausler, C., Balke, H., 2004. Periodic permeable interface cracks in piezoelectric materials. International Journal of Solids and Structures 41, 323–335.
Hao, T.F., 2001. Periodical collinear air containing cracks in a piezoelectric material. International Journal of Fracture 112, 197–204.
Jin, B., Zhong, Z., 2002. A moving mode-III crack in functionally graded piezoelectric material: permeable problem. Mechanics Research Communication 29, 217–224.
Kwon, S.M., 2003. Electrical nonlinear anti-plane shear crack in a functionally graded piezoelectric strip. International Journal of Solids and Structures 40, 5649–5667.
Kwon, S.M., Lee, K.Y., 2001. Edge cracked piezoelectric ceramic block under electromechanical impact loading. International Journal of Fracture 112, 139–150.
Li, C.Y., Weng, G.J., 2002. Yoffe-type moving crack in a functionally graded piezoelectric material. Proc. R. Soc. Lond. A 458, 381–399.
Meguid, S.A., Chen, Z.T., 2001. Transient response of finite piezoelectric strip containing coplanar insulating cracks under electromechanical impact. Mechanics of Materials 33, 85–96.
Pak, Y.E., 1990. Crack extension force in a piezoelectric material. Journal of Applied Mechanics 57, 647–653.
Park, S.B., Sun, C.T., 1995. Fracture criteria for piezoelectric ceramics. Journal of the American Ceramic Society 78, 1475–1480.
Sih, G.C., Zuo, J.Z., 2000. Multiscale behavior of crack initiation and growth in piezoelectric ceramics. Theoretical and Applied Fracture Mechanics 34, 123–141.
Soh, A.K., Fang, D.N., Lee, K.L., 2001. Fracture analysis of piezoelectric materials with defects using energy density theory. International Journal of Solids and Structures 38, 8305–8318.
Sosa, H., 1991. Plane problems in piezoelectric media with defects. International Journal of Solids and Structures 28, 491–505.
Sosa, H., Khutoryansky, N., 1996. New developments concerning piezoelectric materials with defects. International Journal of Solids and Structures 33, 3399–3414.
Suo, Z., Kuo, C.M., Barnett, D.M., Willis, J.R., 1992. Fracture mechanics for piezoelectric ceramics. Journal of the Mechanics and Physics of Solids 40, 739–765.
Ueda, S., 2003. Crack in functionally graded piezoelectric strip bonded to elastic surface layers under electromechanical loading. Theoretical and Applied Fracture Mechanics 40, 225–236.
Wang, B.L., Noda, N., 2001. Thermally induced fracture of a smart functionally graded composite structure. Theoretical and Applied Fracture Mechanics 35, 93–109.
Wang, X.Y., Yu, S.W., 2000. Transient response of a crack in a piezoelectric strip objected to the mechanical and electrical impacts: mode III problem. International Journal of Solids and Structures 37, 5795–5808.
Wu, C.M., Kahn, M.K., Moy, W., 1996. Piezoelectric ceramics with functionally gradients: a new application in material design. Journal of the American Ceramic Society 79, 809–812.
Zhu, X., Xu, J., Meng, Z., 2000. Microdisplacement characteristics and microstructures of functionally gradient piezoelectric ceramic actuator. Materials Design 21, 561–566.
Zuo, J.Z., Sih, G.C., 2000. Energy density formulation and interpretation of cracking behavior for piezoelectric ceramics. Theoretical and Applied Fracture Mechanics 34, 17–33.